

## IMPROVED ANTENNA ARRAY ADAPTIVE BEAMFORMING WITH LOW SIDE LOBE LEVEL USING A NOVEL ADAPTIVE INVASIVE WEED OPTIMIZATION METHOD

Z. D. Zaharis<sup>1, \*</sup>, C. Skeberis<sup>2</sup>, and T. D. Xenos<sup>2</sup>

<sup>1</sup>Telecommunications Center, Aristotle University of Thessaloniki, Thessaloniki 54124, Greece

<sup>2</sup>Department of Electrical and Computer Engineering, Aristotle University of Thessaloniki, Thessaloniki 54124, Greece

**Abstract**—An improved adaptive beamforming technique of antenna arrays is introduced. The technique is implemented by using a novel Invasive Weed Optimization (IWO) variant called Adaptive Dispersion Invasive Weed Optimization (ADIWO) where the seeds produced by a weed are dispersed in the search space with standard deviation specified by the fitness value of the weed. The adaptive seed dispersion makes the ADIWO converge faster than the conventional IWO. This behavior is verified by applying both the ADIWO and the conventional IWO on well-known test functions. The ADIWO method is utilized here as an adaptive beamformer that makes a uniform linear antenna array steer the main lobe towards the direction of arrival (DoA) of a desired signal, form nulls towards the respective DoA of several interference signals and achieve low side lobe level (*SLL*). The proposed ADIWO based beamformer is compared to a Particle Swarm Optimization (PSO) based beamformer and a well known beamforming method called Minimum Variance Distortionless Response (MVDR). Several cases have been studied with different number of interference signals and different power level of additive zero-mean Gaussian noise. The results show that the ADIWO provides sufficient steering ability regarding the main lobe and the nulls, works faster than the PSO and achieves better *SLL* than the PSO and MVDR.

---

*Received 2 December 2011, Accepted 9 January 2012, Scheduled 17 January 2012*

\* Corresponding author: Zaharias D. Zaharis (zaharis@auth.gr).

## 1. INTRODUCTION

Modern communications involve many new and challenging issues, especially those concerning smart antennas [1–5]. Antenna array beamforming is one of them [5–18]. It helps the array improve the reception of any desired signal and also reduce the reception of any interference or other undesired signal, improving thus the signal-to-interference ratio (SIR). To cope with that, an adaptive beamformer has to calculate the array excitation weights that steer the main lobe towards the direction of arrival (DoA) of the desired signal and create a pattern null towards the DoA of every undesired or interference signal. In practice, the above calculation is a real time procedure, since the DoA of all the incoming signals change with time. Therefore, the calculation must be completed as soon as possible.

Many adaptive beamforming (ABF) techniques have been proposed so far in order to optimize the steering ability of the array regarding the main lobe and the nulls and therefore improve the signal-to-interference-plus-noise ratio (SINR). Such a technique is the Minimum Variance Distortionless Response (MVDR) [2, 16]. Nevertheless, a radiation pattern with low side lobe level (*SLL*) is also desirable since it avoids an unreasonable spatial spread of radiated power. A conventional ABF technique like MVDR aims at improving the SINR but it cannot minimize the *SLL*. To maximize the SINR and also minimize the *SLL*, several evolutionary optimization methods have been introduced and applied as adaptive beamformers with great success [3, 12–14, 18]. The basic drawback of such methods is the increased computational time which is a prohibitive factor for real time techniques. Therefore, a fast evolutionary method would be more suitable for ABF applications.

In the present paper, the authors introduce an improved variant of the recently proposed Invasive Weed Optimization (IWO) [18–26] called Adaptive Dispersion Invasive Weed Optimization (ADIWO). The ADIWO algorithm is based on the IWO source code provided by Mehrabian and Lucas [19]. The main difference between the IWO and the ADIWO lies in the way the seeds produced by a weed are dispersed in the search space. In the conventional IWO, the standard deviation of the seed dispersion decreases as a function of the number of iterations and is the same for all the seeds at a given iteration. However, in the ADIWO, the standard deviation of the dispersion of the seeds produced by a weed is a function of the fitness value of this weed. The adaptive seed dispersion makes the ADIWO converge faster than the conventional IWO. This behavior is verified by applying both the ADIWO and IWO on well-known test functions [27].

The ADIWO algorithm is utilized here as an adaptive beamformer, which optimizes the steering ability of uniform linear arrays (ULAs) regarding the main lobe and the nulls and also achieves low *SLL*. The ADIWO based beamformer is compared to a Particle Swarm Optimization (PSO) based beamformer and the MVDR technique. The input data for all the beamformers are the signal-to-noise ratio (*SNR*) and the DoA of the incoming signals. These directions are considered to be already estimated by well-known DoA algorithms [28–34]. Due to uncertainties in the amplitudes of the interference signals that may be observed in practice, the exact element values of the interference correlation matrix are not taken into account. Therefore, the interference correlation matrix is taken as the identity matrix. Several cases have been studied with different number of interference signals and different power level of additive zero-mean Gaussian noise. The results show that the ADIWO provides sufficient steering ability regarding the main lobe and the nulls, works faster than the PSO and achieves better *SLL* than the PSO and MVDR.

## 2. BEAMFORMING PROBLEM FORMULATION

The beamforming problem has already been described in [12]. A ULA of  $M$  monochromatic isotropic elements receives a desired signal  $s$  from angle of arrival (AoA)  $\theta_0$  and  $N$  interference signals  $i_n$  ( $n = 1, \dots, N$ ) arriving respectively from  $\theta_n$  ( $n = 1, \dots, N$ ), in the presence of additive zero-mean Gaussian noise with variance  $\sigma_{noise}^2$ . Each  $\theta_n$  ( $n = 0, 1, \dots, N$ ) is defined by the DoA of  $s$  or  $i_n$  and the normal to the array axis direction. The signals  $s$ ,  $i_n$  ( $n = 1, \dots, N$ ) and the noise signals are all uncorrelated with each other. The quiescent pattern (QP) of the array is derived when all the excitation weights are of equal amplitude and phase. This pattern has to be modified in order to steer the main lobe towards  $\theta_0$ , place nulls towards  $\theta_n$  ( $n = 1, \dots, N$ ) and achieve low *SLL*.

According to the formulation of the beamforming problem given in [12], the steering ability of the ULA regarding the main lobe and the nulls is optimized by minimizing the fitness function given below:

$$F = \frac{\bar{w}^H \bar{A} \bar{A}^H \bar{w} + \sigma_{noise}^2 \bar{w}^H \bar{w}}{\bar{w}^H \bar{a}_0 \bar{a}_0^H \bar{w}} \quad (1)$$

where

$$\bar{w} = [w_1 \quad w_2 \quad \dots \quad w_M]^T \quad (2)$$

$$\bar{A} = [\bar{a}_1 \quad \bar{a}_2 \quad \dots \quad \bar{a}_N] \quad (3)$$

$$\bar{a}_n = \left[ 1 \quad e^{j \frac{2\pi}{\lambda} q \sin \theta_n} \quad \dots \quad e^{j(M-1) \frac{2\pi}{\lambda} q \sin \theta_n} \right]^T, \quad n = 0, 1, \dots, N \quad (4)$$

are, respectively, the vector of the ULA excitation weights, the  $M \times N$  array steering matrix, and the array steering vector that corresponds to AoA  $\theta_n$ . Also,  $q$  is the distance between adjacent elements of the ULA, while the superscripts  $T$  and  $H$  imply the transpose matrix and the Hermitian transpose matrix, respectively. The consideration about the interference correlation matrix, which is taken as the identity matrix as explained in the previous section, has already been taken into account in (1). In order to satisfy the additional requirement for low  $SLL$ , the fitness function expression must be modified as follows:

$$F = bf_1 \frac{\bar{w}^H \bar{A} \bar{A}^H \bar{w} + \sigma_{noise}^2 \bar{w}^H \bar{w}}{\bar{w}^H \bar{a}_0 \bar{a}_0^H \bar{w}} + bf_2 SLL \quad (5)$$

The factors  $bf_1$  and  $bf_2$  are used to balance the minimization of the two terms shown in (5). The fitness function as given in (5) is used by both the ADIWO-based and PSO-based beamformers to estimate the respective array excitation weights. The calculation of the excitation weights using the MVDR technique is also described in [12].

### 3. ADAPTIVE DISPERSION IWO

The original IWO method was initially proposed by Mehrabian and Lucas in [19]. Since then, several studies have been published on antenna design using IWO [18, 20–22, 24, 25]. In addition, several efficient IWO variants have been proposed [23, 26]. Nevertheless, the original IWO and all the IWO variants proposed so far have a common feature concerning the way the seeds produced by a weed are dispersed in the search space: The standard deviation of the seed dispersion  $\sigma$  decreases as a function of the number of iterations  $iter$ . Obviously, the value of  $\sigma$  defines the exploration ability of the weeds. Therefore, as  $iter$  increases, the exploration ability of all the weeds is gradually reduced. At the end of the optimization process, the exploration ability has diminished so much that every weed can only fine tune its position. Then, if the optimal position has not been found yet, it will never be found.

In the ADIWO, the standard deviation  $\sigma$  of the dispersion of the seeds produced by a weed is a linear function of the fitness value  $f$  of this weed. Considering that the goal is the minimization of the fitness function,  $\sigma$  can be estimated according to the following expression:

$$\sigma = \frac{\sigma_{\max} - \sigma_{\min}}{f_{\max} - f_{\min}} f + \frac{\sigma_{\min} f_{\max} - \sigma_{\max} f_{\min}}{f_{\max} - f_{\min}} \quad (6)$$

where  $\sigma_{\max}$  and  $\sigma_{\min}$  are the standard deviation limits defined in the same way as in the original IWO algorithm, while  $f_{\max}$  and  $f_{\min}$

represent respectively the maximum and minimum fitness values at a certain iteration. The ADIWO algorithm has the same structure as the original IWO algorithm described in [19]. The only difference lies in the calculation of  $\sigma$  which is performed by using (6). It is easy to realize that the best weed ( $f = f_{\min}$ ) disperses its seeds with the minimum  $\sigma$  ( $\sigma = \sigma_{\min}$ ), while the worst weed ( $f = f_{\max}$ ) disperses its seeds with the maximum  $\sigma$  ( $\sigma = \sigma_{\max}$ ). Therefore, the weeds have different behavior depending on their fitness values. As the fitness value gets closer to  $f_{\min}$ , the exploration ability of the weed is reduced and thus the weed can only fine tune its near-optimal position. On the contrary, as  $f$  gets closer to  $f_{\max}$ , the exploration ability of the weed increases and thus the weed is capable of exploring the search space to find better positions. In this way, the exploration ability of the weed colony is maintained until the end of the optimization process. Moreover, the adaptive seed dispersion makes the ADIWO converge faster than the original IWO. This behavior is verified in the next section.

#### 4. CONVERGENCE RESULTS

The ADIWO was compared to the original IWO in terms of convergence. Both algorithms were applied to minimize two well-known test functions, i.e., the generalized Rastrigin function and the generalized Rosenbrock function [27]. Both functions were applied in 30 dimensions. For each function, the ADIWO and IWO algorithms were executed 100 times in order to extract comparative graphs that display the average convergence. For both algorithms, the population size is limited to 30 weeds, the number of seeds produced by a weed ranges from 5 to zero depending on the fitness value of the weed, and finally the standard deviation limits are  $\sigma_{\max} = 10$  and  $\sigma_{\min} = 0.5$ . The comparative graphs given in Figures 1 and 2 show that both algorithms result in the same solutions. However, the ADIWO

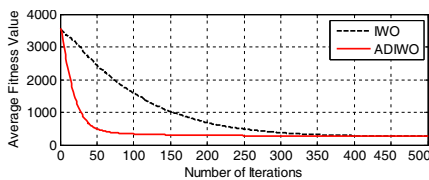


**Figure 1.** Comparative convergence graphs for 30-D Rastrigin function.

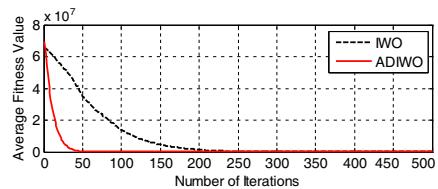


**Figure 2.** Comparative convergence graphs for 30-D Rosenbrock function.

algorithm outperforms the IWO algorithm regarding the convergence speed. Due to its fast convergence, the ADIWO algorithm is suitable for real time applications like ABF.

## 5. ADAPTIVE BEAMFORMING EXAMPLES

The ADIWO algorithm was applied as an ABF technique on a 9-element ULA ( $M = 9$ ), with  $q = 0.5\lambda$ , in comparison to a PSO-based beamformer and the MVDR technique. The parameter values concerning the ADIWO algorithm are the same as in the previous section. The PSO algorithm used here is a PSO variant known as Constriction Factor PSO (CFPSO) [35]. In this algorithm, the parameters  $c_1$  and  $c_2$  are set equal to 2.05 and thus the constriction factor  $K$  calculated by (6) in [35] is found equal to 0.7298. In addition, both the CFPSO and the ADIWO use the same population size (i.e., 30 particles) and take 500 iterations to complete each execution.

In all the ABF cases studied here, the algorithms were executed on an Intel Core i5 computer running Microsoft Windows 7. The mean CPU time per execution required by the ADIWO algorithm was found 250 times less than the corresponding time required by the PSO algorithm. Due to the short execution time and the fast convergence, the ADIWO algorithm is more suitable for real time applications than other evolutionary optimization methods, such as the PSO.

The three ABF algorithms were applied to four sets of 100 random cases per set. Each case is a group of  $N + 1$  random values different

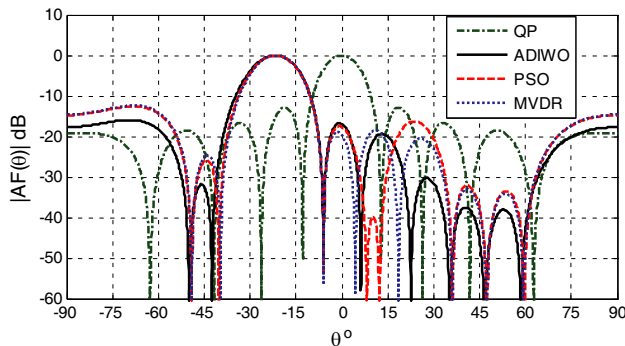


**Figure 3.** Optimal radiation patterns for  $SNR = 10$  dB, a desired signal arriving from  $\theta_0 = -22^\circ$ , and five interference signals arriving from  $\theta_1 = -49^\circ$ ,  $\theta_2 = -6^\circ$ ,  $\theta_3 = 36^\circ$ ,  $\theta_4 = 47^\circ$  and  $\theta_5 = 59^\circ$  (derived  $SLL$  values:  $SLL_{qp} = -12.90$  dB,  $SLL_{adiwo} = -15.96$  dB,  $SLL_{pso} = -12.59$  dB,  $SLL_{mvdr} = -12.40$  dB).

from each other given to  $\theta_n$  ( $n = 0, 1, \dots, N$ ). The first two sets use five interference signals ( $N = 5$ ) and refer respectively to  $SNR = 10$  dB and  $SNR = 30$  dB. Also, the last two sets use seven interference signals ( $N = 7$ ) and refer respectively to  $SNR = 10$  dB and  $SNR = 30$  dB. For each random case, the algorithms are applied to find the near-optimal excitation vectors, respectively  $\bar{w}_{adiwo}$ ,  $\bar{w}_{pso}$  and  $\bar{w}_{mvdr}$ , that produce a main lobe towards the AoA  $\theta_0$  of the desired signal,  $N$  nulls towards

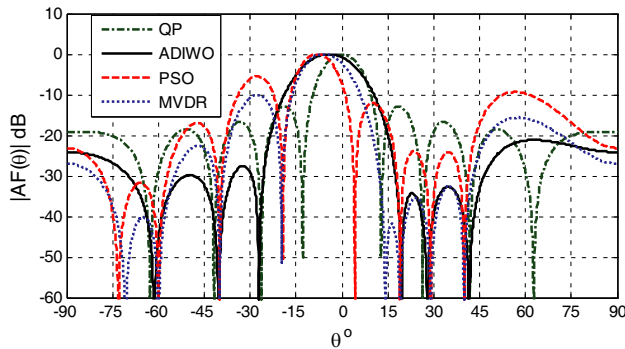


**Figure 4.** Optimal radiation patterns for  $SNR = 30$  dB, a desired signal arriving from  $\theta_0 = -5^\circ$ , and five interference signals arriving from  $\theta_1 = -60^\circ$ ,  $\theta_2 = -40^\circ$ ,  $\theta_3 = 19^\circ$ ,  $\theta_4 = 28^\circ$  and  $\theta_5 = 40^\circ$  (derived  $SLL$  values:  $SLL_{qp} = -12.90$  dB,  $SLL_{adiwo} = -21.18$  dB,  $SLL_{pso} = -5.52$  dB,  $SLL_{mvdr} = -10.06$  dB).

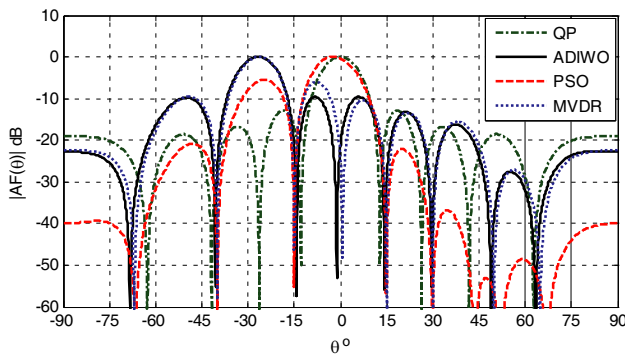


**Figure 5.** Optimal radiation patterns for  $SNR = 10$  dB, a desired signal arriving from  $\theta_0 = -25^\circ$ , and seven interference signals arriving from  $\theta_1 = -67^\circ$ ,  $\theta_2 = -40^\circ$ ,  $\theta_3 = -15^\circ$ ,  $\theta_4 = 15^\circ$ ,  $\theta_5 = 30^\circ$ ,  $\theta_6 = 50^\circ$  and  $\theta_7 = 65^\circ$  (derived  $SLL$  values:  $SLL_{qp} = -12.90$  dB,  $SLL_{adiwo} = -9.57$  dB,  $SLL_{pso} = -5.49$  dB,  $SLL_{mvdr} = -6.01$  dB).

the AoA  $\theta_n$  ( $n = 1, \dots, N$ ) of the interference signals and, if possible, minimize the  $SLL$ . Then, the vectors  $\bar{w}_{adiwo}$ ,  $\bar{w}_{pso}$  and  $\bar{w}_{mvdr}$  are used to produce the respective radiation patterns and thus calculate the corresponding angular deviations  $\Delta\theta_{adiwo}^{main}$ ,  $\Delta\theta_{pso}^{main}$  and  $\Delta\theta_{mvdr}^{main}$  of the main lobe direction from its desired value  $\theta_0$ , the angular deviations  $\Delta\theta_{adiwo}^{null}$ ,  $\Delta\theta_{pso}^{null}$  and  $\Delta\theta_{mvdr}^{null}$  of the null directions from their respective desired values  $\theta_n$  ( $n = 1, \dots, N$ ), and the corresponding side lobe levels

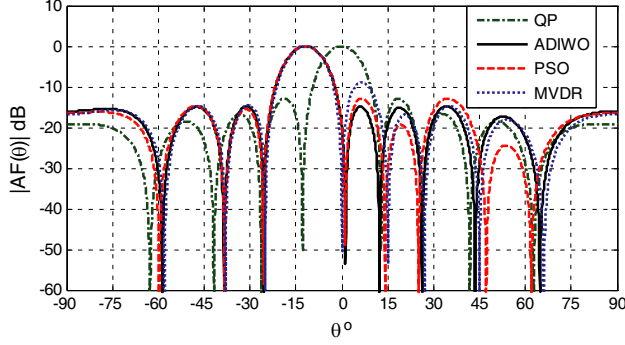


**Figure 6.** Optimal radiation patterns for  $SNR = 30$  dB, a desired signal arriving from  $\theta_0 = -11^\circ$ , and seven interference signals arriving from  $\theta_1 = -58^\circ$ ,  $\theta_2 = -38^\circ$ ,  $\theta_3 = -25^\circ$ ,  $\theta_4 = 0^\circ$ ,  $\theta_5 = 27^\circ$ ,  $\theta_6 = 44^\circ$  and  $\theta_7 = 65^\circ$  (derived  $SLL$  values:  $SLL_{qp} = -12.90$  dB,  $SLL_{adiwo} = -14.82$  dB,  $SLL_{pso} = -12.87$  dB,  $SLL_{mvdr} = -9.02$  dB).

**Table 1.** Statistical analysis performed on the ABF results.

Set	1st	2nd	3rd	4th
$SNR$	10 dB	30 dB	10 dB	30 dB
$N$	5	5	7	7
$\Delta\theta_{adiwo}^{main}$	$0.64^\circ$	$1.50^\circ$	$1.41^\circ$	$1.42^\circ$
$\Delta\theta_{pso}^{main}$	$0.62^\circ$	$1.47^\circ$	$1.44^\circ$	$1.39^\circ$
$\Delta\theta_{mvdr}^{main}$	$0.62^\circ$	$0.96^\circ$	$1.39^\circ$	$1.10^\circ$
$\Delta\theta_{adiwo}^{null}$	$0.20^\circ$	$0.18^\circ$	$0.29^\circ$	$0.28^\circ$
$\Delta\theta_{pso}^{null}$	$0.17^\circ$	$0.14^\circ$	$0.26^\circ$	$0.24^\circ$
$\Delta\theta_{mvdr}^{null}$	$0.16^\circ$	$0.10^\circ$	$0.17^\circ$	$0.15^\circ$
$\overline{SLL}_{adiwo}$	-12.87 dB	-14.78 dB	-10.75 dB	-13.99 dB
$\overline{SLL}_{pso}$	-11.53 dB	-11.34 dB	-9.72 dB	-11.76 dB
$\overline{SLL}_{mvdr}$	-11.49 dB	-11.25 dB	-9.62 dB	-11.57 dB



$SLL_{adiwo}$ ,  $SLL_{pso}$  and  $SLL_{mvdrr}$ . Finally, the average absolute angular deviation values  $\overline{\Delta\theta}_{adiwo}^{main}$ ,  $\overline{\Delta\theta}_{pso}^{main}$  and  $\overline{\Delta\theta}_{mvdrr}^{main}$  concerning the main lobe direction, the average absolute angular deviation values  $\overline{\Delta\theta}_{adiwo}^{null}$ ,  $\overline{\Delta\theta}_{pso}^{null}$  and  $\overline{\Delta\theta}_{mvdrr}^{null}$  concerning the null directions, and the average  $SLL$  values  $\overline{SLL}_{adiwo}$ ,  $\overline{SLL}_{pso}$  and  $\overline{SLL}_{mvdrr}$  are calculated for each set of 100 random cases. The statistical analysis performed on the ABF results is given in Table 1. It is obvious that the ADIWO provides

**Table 2.** Optimal excitation weight values for  $SNR = 10$  dB, a desired signal arriving from  $\theta_0 = -22^\circ$ , and five interference signals arriving from  $\theta_1 = -49^\circ$ ,  $\theta_2 = -6^\circ$ ,  $\theta_3 = 36^\circ$ ,  $\theta_4 = 47^\circ$  and  $\theta_5 = 59^\circ$ .

$m$	$w_{adiwo}$	$w_{pso}$	$w_{mvdrr}$
1	$-0.059-j0.356$	$-0.028-j0.516$	$-0.057-j0.467$
2	$-0.614-j0.195$	$-0.657-j0.167$	$-0.627-j0.176$
3	$-0.459+j0.426$	$-0.385+j0.595$	$-0.324+j0.443$
4	$0.215+j0.783$	$0.128+j1.000$	$0.195+j0.796$
5	$1.000+j0$	$1.000+j0$	$1.000+j0$
6	$0.215-j0.783$	$0.128-j1.000$	$0.195-j0.796$
7	$-0.459-j0.426$	$-0.385-j0.595$	$-0.324-j0.443$
8	$-0.614+j0.195$	$-0.657+j0.167$	$-0.627+j0.176$
9	$-0.059+j0.356$	$-0.028+j0.516$	$-0.057+j0.467$

**Table 3.** Optimal excitation weight values for  $SNR = 30$  dB, a desired signal arriving from  $\theta_0 = -5^\circ$ , and five interference signals arriving from  $\theta_1 = -60^\circ$ ,  $\theta_2 = -40^\circ$ ,  $\theta_3 = 19^\circ$ ,  $\theta_4 = 28^\circ$  and  $\theta_5 = 40^\circ$ .

$m$	$w_{adiwo}$	$w_{pso}$	$w_{mvdrr}$
1	$0.046+j0.049$	$-0.513+j1.141$	$-0.063+j0.442$
2	$0.309+j0.280$	$0.401+j1.168$	$0.421+j0.509$
3	$0.577+j0.254$	$1.263+j1.062$	$0.929+j0.447$
4	$0.976+j0.220$	$0.500-j0.024$	$0.795+j0.036$
5	$1.000+j0$	$1.000+j0$	$1.000+j0$
6	$0.976-j0.220$	$0.500+j0.024$	$0.795-j0.036$
7	$0.577-j0.254$	$1.263-j1.062$	$0.929-j0.447$
8	$0.309-j0.280$	$0.401-j1.168$	$0.421-j0.509$
9	$0.046-j0.049$	$-0.513-j1.141$	$-0.063-j0.442$

sufficient steering ability regarding the main lobe and the nulls, and achieves better *SLL* than the PSO and MVDR. This is also shown in Figures 3–6, which display the optimal radiation patterns of four typical cases chosen respectively from the four sets mentioned above. The optimal excitation weights are given respectively in Tables 2–5.

**Table 4.** Optimal excitation weight values for  $SNR = 10$  dB, a desired signal arriving from  $\theta_0 = -25^\circ$ , and seven interference signals arriving from  $\theta_1 = -67^\circ$ ,  $\theta_2 = -40^\circ$ ,  $\theta_3 = -15^\circ$ ,  $\theta_4 = 15^\circ$ ,  $\theta_5 = 30^\circ$ ,  $\theta_6 = 50^\circ$  and  $\theta_7 = 65^\circ$ .

$m$	$w_{adiwo}$	$w_{pso}$	$w_{mvdr}$
1	0.894–j1.022	0.274+j0.477	1.119–j1.634
2	–0.284–j1.428	1.372+j0.690	–0.593–j2.135
3	–0.974+j0.456	1.886–j0.072	–1.542+j0.477
4	0.322+j0.876	1.344–j0.428	0.129+j1.020
5	1.000+j0	1.000+j0	1.000+j0
6	0.322–j0.876	1.344+j0.428	0.129–j1.020
7	–0.974–j0.456	1.886+j0.072	–1.542–j0.477
8	–0.284+j1.428	1.372–j0.690	–0.593+j2.135
9	0.894+j1.022	0.274–j0.477	1.119+j1.634

**Table 5.** Optimal excitation weight values for  $SNR = 30$  dB, a desired signal arriving from  $\theta_0 = -11^\circ$ , and seven interference signals arriving from  $\theta_1 = -58^\circ$ ,  $\theta_2 = -38^\circ$ ,  $\theta_3 = -25^\circ$ ,  $\theta_4 = 0^\circ$ ,  $\theta_5 = 27^\circ$ ,  $\theta_6 = 44^\circ$  and  $\theta_7 = 65^\circ$ .

$m$	$w_{adiwo}$	$w_{pso}$	$w_{mvdr}$
1	–0.881+j0.566	–1.000+j0.694	–1.101+j0.943
2	–0.282+j0.739	–0.367+j1.000	–0.425+j1.169
3	0.256+j0.823	0.344+j1.000	0.202+j1.207
4	0.826+j0.633	1.000+j1.000	0.841+j0.921
5	1.000+j0	1.000+j0	1.000+j0
6	0.826–j0.633	1.000–j1.000	0.841–j0.921
7	0.256–j0.823	0.344–j1.000	0.202–j1.207
8	–0.282–j0.739	–0.367–j1.000	–0.425–j1.169
9	–0.881–j0.566	–1.000–j0.694	–1.101–j0.943

## 6. CONCLUSION

A robust ABF technique based on the ADIWO method has been presented. The ADIWO is a novel optimization method based on the recently proposed IWO and improved by incorporating an adaptive seed dispersion mechanism. A comparative study applied on well-known test functions reveals the superiority of this mechanism regarding the convergence speed. By recording the CPU time in four sets of 100 ABF cases per set, the ADIWO algorithm seems to be much faster than the PSO algorithm. Both the increased convergence speed and the short execution time make the ADIWO algorithm more suitable for real time applications, like ABF, than other evolutionary optimization algorithms. The ABF cases studied in the present paper take into account the knowledge of the DoA of all the signals received by the antenna array. However, the interference correlation matrix is not used here, considering uncertainties in the amplitudes of the interference signals that may be observed in practice. The statistical analysis performed on the ABF results shows that the ADIWO-based beamformer provides sufficient steering ability regarding the main lobe and the nulls, and also achieves better *SLL* than the PSO-based beamformer and the MVDR. Therefore, the ADIWO method seems to be very useful in ABF applications.

## ACKNOWLEDGMENT

The authors would like to thank Dr. A. R. Mehrabian for providing the source code of the IWO algorithm.

## REFERENCES

1. Godara, L. C., *Smart Antennas*, CRC Press, Boca Raton, FL, 2004.
2. Gross, F. B., *Smart Antennas for Wireless Communications with Matlab*, McGraw-Hill, New York, 2005.
3. Ho, M.-H., S.-H. Liao, and C.-C. Chiu, "A novel smart UWB antenna array design by PSO," *Progress In Electromagnetics Research C*, Vol. 15, 103–115, 2010.
4. Viani, F., L. Lizzi, M. Donelli, D. Pregnotato, G. Oliveri, and A. Massa, "Exploitation of parasitic smart antennas in wireless sensor networks," *Journal of Electromagnetic Waves and Applications*, Vol. 24, No. 7, 993–1003, 2010.

5. Jabbar, A. N., "A novel ultra-fast ultra-simple adaptive blind beamforming algorithm for smart antenna arrays," *Progress In Electromagnetics Research B*, Vol. 35, 329–348, 2011.
6. Li, J. and P. Stoica, *Robust Adaptive Beamforming*, John Wiley & Sons, Inc., Hoboken, New Jersey, 2006.
7. Castaldi, G., V. Galdi, and G. Gerini, "Evaluation of a neural-network-based adaptive beamforming scheme with magnitude-only constraints," *Progress In Electromagnetics Research B*, Vol. 11, 1–14, 2009.
8. Umrani, A. W., Y. Guan, and F. A. Umrani, "Effect of steering error vector and angular power distributions on beamforming and transmit diversity systems in correlated fading channel," *Progress In Electromagnetics Research*, Vol. 105, 383–402, 2010.
9. Byrne, D., M. O'Halloran, M. Glavin, and E. Jones, "Data independent radar beamforming algorithms for breast cancer detection," *Progress In Electromagnetics Research*, Vol. 107, 331–348, 2010.
10. Byrne, D., M. O'Halloran, E. Jones, and M. Glavin, "Transmitter-grouping robust capon beamforming for breast cancer detection," *Progress In Electromagnetics Research*, Vol. 108, 401–416, 2010.
11. Lee, J.-H., Y.-S. Jeong, S.-W. Cho, W.-Y. Yeo, and K. S. J. Pister, "Application of the newton method to improve the accuracy of toa estimation with the beamforming algorithm and the music algorithm," *Progress In Electromagnetics Research*, Vol. 116, 475–515, 2011.
12. Zaharis, Z. D. and T. V. Yioultsis, "A novel adaptive beamforming technique applied on linear antenna arrays using adaptive mutated boolean PSO," *Progress In Electromagnetics Research*, Vol. 117, 165–179, 2011.
13. Mallipeddi, R., J. P. Lie, P. N. Suganthan, S. G. Razul, and C. M. S. See, "A differential evolution approach for robust adaptive beamforming based on joint estimation of look direction and array geometry," *Progress In Electromagnetics Research*, Vol. 119, 381–394, 2011.
14. Mallipeddi, R., J. P. Lie, P. N. Suganthan, S. G. Razul, and C. M. S. See, "Near optimal robust adaptive beamforming approach based on evolutionary algorithm," *Progress In Electromagnetics Research B*, Vol. 29, 157–174, 2011.
15. Wang, W., R. Wu, and J. Liang, "A novel diagonal loading method for robust adaptive beamforming," *Progress In Electromagnetics Research C*, Vol. 18, 245–255, 2011.

16. Liu, F., J. Wang, C. Y. Sun, and R. Du, "Robust MVDR beamformer for nulling level control via multi-parametric quadratic programming," *Progress In Electromagnetics Research C*, Vol. 20, 239–254, 2011.
17. Mallipeddi, R., J. P. Lie, S. G. Razul, P. N. Suganthan, and C. M. S. See, "Robust adaptive beamforming based on covariance matrix reconstruction for look direction mismatch," *Progress In Electromagnetics Research Letters*, Vol. 25, 37–46, 2011.
18. Roshanaei, M., C. Lucas, and A. R. Mehrabian, "Adaptive beamforming using a novel numerical optimisation algorithm," *IET Microwaves, Antennas & Propagation*, Vol. 3, No. 5, 765–773, Aug. 2009.
19. Mehrabian, A. R. and C. Lucas, "A novel numerical optimization algorithm inspired from weed colonization," *Ecological Informatics*, Vol. 1, 355–366, 2006.
20. Mallahzadeh, A. R., H. Oraizi, and Z. Davoodi-Rad, "Application of the invasive weed optimization technique for antenna configurations," *Progress In Electromagnetics Research*, Vol. 79, 137–150, 2008.
21. Mallahzadeh, A. R., S. Es'haghi, and A. Alipour, "Design of an E-shaped MIMO antenna using IWO algorithm for wireless application at 5.8 GHz," *Progress In Electromagnetics Research*, Vol. 90, 187–203, 2009.
22. Karimkashi, S. and A. A. Kishk, "Invasive weed optimization and its features in electromagnetics," *IEEE Transactions on Antennas and Propagation*, Vol. 58, No. 4, 1269–1278, Apr. 2010.
23. Basak, A., S. Pal, S. Das, and A. Abraham, "Circular antenna array synthesis with a differential invasive weed optimization algorithm," *10th International Conference on Hybrid Intelligent Systems (HIS)*, 153–158, Aug. 23–25, 2010.
24. Monavar, F. M. and N. Komjani, "Bandwidth enhancement of microstrip patch antenna using jerusalem cross-shaped frequency selective surfaces by invasive weed optimization approach," *Progress In Electromagnetics Research*, Vol. 121, 103–120, 2011.
25. Karimkashi, S., A. A. Kishk, and D. Kajfez, "Antenna array optimization using dipole models for MIMO applications," *IEEE Transactions on Antennas and Propagation*, Vol. 59, No. 8, 3112–3116, Aug. 2011.
26. Roy, G. G., S. Das, P. Chakraborty, and P. N. Suganthan, "Design of non-uniform circular antenna arrays using a modified invasive weed optimization algorithm," *IEEE Transactions on Antennas and Propagation*, Vol. 59, No. 1, 110–118, Jan. 2011.

27. Mezura-Montes, E., J. Velázquez-Reyes, and C. A. C. Coello, "A comparative study of differential evolution variants for global optimization," *Proceedings of the 8th Annual Conference on Genetic and Evolutionary Computation (GECCO'06)*, 485–492, 2006.
28. Yang, P., F. Yang, and Z.-P. Nie, "DOA estimation with sub-array divided technique and interpolated esprit algorithm on a cylindrical conformal array antenna," *Progress In Electromagnetics Research*, Vol. 103, 201–216, 2010.
29. Park, G. M., H. G. Lee, and S. Y. Hong, "Doa resolution enhancement of coherent signals via spatial averaging of virtually expanded arrays," *Journal of Electromagnetic Waves and Applications*, Vol. 24, No. 1, 61–70, 2010.
30. Lui, H. S. and H. T. Hui, "Effective mutual coupling compensation for direction-of-arrival estimations using a new, accurate determination method for the receiving mutual impedance," *Journal of Electromagnetic Waves and Applications*, Vol. 24, No. 2–3, 271–281, 2010.
31. Liang, J. and D. Liu, "Two l-shaped array-based 2-D DOAs estimation in the presence of mutual coupling," *Progress In Electromagnetics Research*, Vol. 112, 273–298, 2011.
32. Kim, Y. and H. Ling, "Direction of arrival estimation of humans with a small sensor array using an artificial neural network," *Progress In Electromagnetics Research B*, Vol. 27, 127–149, 2011.
33. Xie, J., Z.-S. He, and H.-Y. Li, "A fast DOA estimation algorithm for uniform circular arrays in the presence of unknown mutual coupling," *Progress In Electromagnetics Research C*, Vol. 21, 257–271, 2011.
34. Bencheikh, M. L. and Y. Wang, "Combined esprit-rootmusic for DOA-dod estimation in polarimetric bistatic MIMO radar," *Progress In Electromagnetics Research Letters*, Vol. 22, 109–117, 2011.
35. Eberhart, R. C. and Y. Shi, "Particle swarm optimization: Developments, applications and resources," *Proceedings of the 2001 Congress on Evolutionary Computation*, Vol. 1, 81–86, 2001.